J Solid State Electrochem (2007) 11:655–666
DOI 10.1007/s10008-006-0221-0

ORIGINAL PAPER

Use of iridium oxide films as hydrogen gas evolution cathodes in aqueous media

L. Declan Burke · Nageb S. Naser · Bernadette M. Ahern

Received: 3 July 2006 / Revised: 13 August 2006 / Accepted: 4 September 2006 / Published online: 15 November 2006
© Springer-Verlag 2006

Abstract Hydrous iridium oxide films are highly resistant to reduction under cathodic, hydrogen gas evolution, conditions in aqueous acid or base. Such behavior is not in agreement with simple thermodynamic (Pourbaix) data based on the assumption that the system behaves in a reversible manner. The barrier to reduction is attributed, as discussed earlier for RuO_2, to the involvement of high-energy intermediates (iridium atoms or microclusters of same) which can only be generated at unusually negative overpotential values evidently far into the hydrogen gas evolution region. Thermally prepared IrO_2/Ti electrodes are possible candidates for hydrogen gas evolution cathodes in water electrolysis cells; however, under extended operating conditions, the performance of these cathodes was found to deteriorate due to gradual shedding of the active oxide layer.

Keywords Iridium · Iridium oxide · Metastability · IrO_2 cathodes · Cathode deterioration

Introduction

The basic cyclic voltammetry behavior of the noble metals in aqueous media has traditionally been discussed [1] in terms of a combination of nonfaradaic (double layer) charging/discharging and surface film (hydride and monolayer, or α, oxide) formation/removal processes. However, there is increasing evidence that such an approach is seriously inadequate as it ignores two important factors: (1) nonequilibrium surface states of metals and (2) the existence of hydrous (or β), as opposed to monolayer (α), oxide films. The nature of metastable metal surface (MMS) states was discussed recently [2, 3] with particular reference to gold; however, the ideas involved are relevant to all noble metal surfaces. It is assumed that there are two extreme, or limiting, surface states, the low-energy equilibrated metal surface (EMS) state and the high-energy MMS state. The difference between them is that the surface atoms involved in the MMS state have a low lattice stabilization energy; this is an intrinsically unstable, poorly ordered (or ill-defined) variable state, whereas the EMS state involves well-embedded metal atoms of high lattice stabilization energy.

A typical metal surface contains elements of both states, usually with the EMS form predominating. Ideal, monatomically flat, single crystal surfaces may be regarded as EMS systems, but a perfect order (or total lack of surface defects) in this area is apparently impossible to achieve [4]. Atoms and minute clusters that are mobile on the surface are at the other extreme; these are very high-energy states, with the atoms involved existing as transient species of low mean coverage. Mobile surface atoms are not imagable by STM; however, their existence is demonstrated by surface dynamic studies [5, 6].

The MMS state (of which the mobile adatom is an extreme form) is assumed to be intrinsically disordered and highly variable. Recent work with gold [2, 3, 7] indicates that severe disruption (or superactivation) of a metal surface can temporally increase the coverage of MMS state, thereby facilitating investigation of the latter. The effect of superactivation can be quite dramatic; a gold surface in aqueous solution usually begins to undergo oxidation [1] at ca. 1.3 V (RHE) but, after superactivation, surface oxidation is observed at a much low potential, ca. 0.3 V [7, 8]; such premonolayer oxidation behavior correlates quite well with the electrocatalytic behavior of gold [7].

L. D. Burke (✉) · N. S. Naser · B. M. Ahern
Chemistry Department, University College Cork,
Cork, Ireland
e-mail: l.d.burke@ucc.ie

Hydrous (β) oxides [9] are quite different in character to their monolayer (α) oxide equivalents (this is discussed in more detail in this study later with regard to iridium). The extent of the deviation from the conventional behavior when β oxide species are involved is often dramatic, e.g., it is possible to produce a gold β oxide film which has a major component that only undergoes reduction (at quite slow sweep rates) in base [2] at ca. −0.2 V (RHE), i.e., at least 1.2 V lower than the α oxide reduction response. The β oxides are low density, hyperextended, ill-defined materials, not unlike (in terms of their disorder) the superactivated state of the metal. Indeed, these two states seem to be closely interrelated, with the MMS/β oxide couple (at low coverages) apparently undergoing a rapid, quasi-reversible redox transition [7] at an unusually low potential where both components of the couple are thermodynamically unstable. As discussed recently for RuO_2 cathodes [10], the sluggish character of the β oxide/metal reduction reaction at high (multilayer) coverages is due to the presence of a high overpotential barrier, the primary product of the reduction reaction being high energy, unusually electropositive, metal atoms, a state that is readily achieved only at unusually low potentials.

There is a considerable interest in the use of some of the rarer noble metal oxides, e.g., RuO_2 and IrO_2, in the energy storage area at the present time. For example, thermally prepared thin films of these materials (on titanium) have been extensively explored as cathodes for use in water electrolysis cells, some of which involve an acidic electrolyte [10–15]. The initial deposits are anhydrous (α-type) oxides but the outer layers undergo hydration (or β oxide formation) at the early stages of the reaction [11]. Furthermore, these oxides, especially RuO_2 (in both anhydrous and hydrated form [16], and often in combination with a less expensive oxide, e.g., NiO [17], TiO_2 [18], and even glassy carbon [19]), have been explored for use in the supercapacitor battery area [20].

Two basic points are of interest here: (1) according to Pourbaix's thermodynamic data [21], iridium and ruthenium have no oxides that are stable with respect to reduction to the metal in aqueous media below ca. 0.93 and 0.74 V (RHE), respectively; yet films of the oxides in question, i.e., IrO_2 and RuO_2, may be used as substrates for hydrogen gas evolution, at $E<0.0$ V, for extended periods of time, apparently without significant signs of deterioration; (2) these oxide deposits exhibit a low hydrogen evolution potential, i.e., they are catalytically active, although (in our experience [10]) the $RuO_2/H_2,H_3O^+$ electrode system shows little sign of reversible behavior, i.e., the mechanism of H_2 evolution catalysis at these oxide electrodes is quite different to that involved in the case of platinum. These two unusual features of noble metal oxide electrochemistry are discussed in the present work which is concerned mainly on the anomalous (or active state) electrochemistry of iridium and its oxides.

Materials and methods

The experiments were carried out using a Metrohm cell (Type EA 880R-20) containing both the working and counter electrode. For work with iridium metal, both electrodes consisted of lengths of iridium wire (Alfa Aesar), typically 0.5 mm diameter and ca. 0.5 cm^2 exposed area, sealed into soda glass. These electrodes were cleaned before use by mild abrasion with Emery paper and washing with distilled water. IrO_2-coated titanium electrodes were prepared by conventional techniques [22, 23]. Titanium wires, 1 mm diameter, were degreased with acetone, etched for 10 min in aqua regia at 40 °C, and washed with distilled water. Ir $Cl_3 \times H_2O$ (Aldrich) was dissolved in 25% HCl (0.1 g per 100 ml), and the solution evaporated almost to dryness. The resulting material was taken up in a small volume of isopropanol to form a paste which was painted onto the titanium surface. The film was dried at 50 °C for 10 min and then heated in air at 550 °C, again for 10 min. This coating process was repeated; a total of four coats were normally applied, and the final heat treatment was extended for a period of 4 h. The coated electrode was sealed, using Araldite, into the end of a glass tube leaving an exposed section, ca. 3 cm long, of IrO_2-coated Ti wire.

Electrode potentials were measured with respect to either reversible hydrogen in the same solution or saturated calomel. The reference electrode was contained in a separate vessel which was connected to the main vessel by a Luggin capillary whose tip was positioned ca. 1 mm away from the surface of the working electrode. Both vessels were suspended in a thermostatted (±0.1 °C) water bath. Solutions were made up using Analar grade chemicals and triply distilled water and were regularly purged with pure nitrogen gas to remove dissolved oxygen; all current densities are given with respect to geometric surface area.

Potential control was maintained using either an analogue system (Wenking LM 81 M potentiostat, Wenking MVS 87 voltage scanner, Goerz, Servogar 790, X-Y recorder) or, for the work with IrO_2, a digital system (CH Instruments, Model 660 B).

Results

Behavior of β oxide films in aqueous acid media

Typical cyclic voltammograms for initially β oxide-free iridium electrodes in acid solution are shown in Fig. 1. Two rather poorly defined pairs of peaks, evidently due to

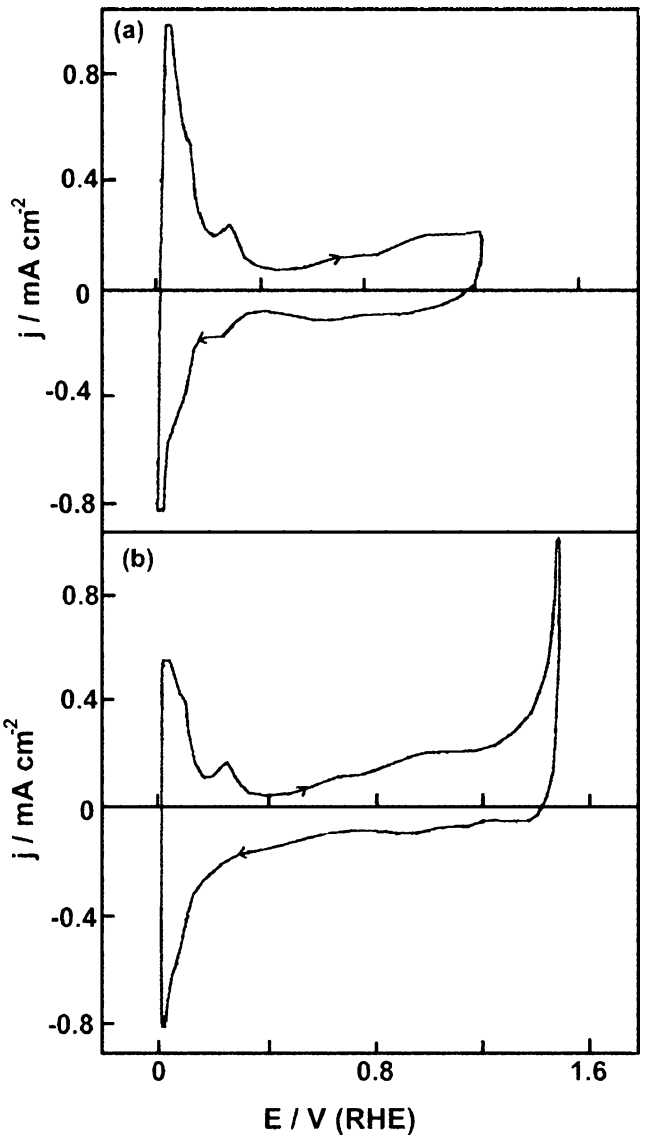

Fig. 1 Cyclic voltammograms (50 mV s^{-1}) for a clean, uncycled, iridium electrode in deoxygenated 1.0 mol dm^{-3} H_2SO_4 at 25 °C. **a** 0.0 to 1.2 V. **b** 0.0 to 1.5 V

reversible adsorption/desorption of hydrogen, one at ca. 0.10 V and the other at ca. 0.26 V, are evident in Fig. 1a. In the latter, a minimum anodic response occurred over the range 0.4–0.5 V (positive sweep), the dominant reaction in this region being double layer charging. Surface oxidation (or α oxide formation) commenced at ca. 0.5 V, but the reaction was sluggish. It extended over much of the positive sweep, with two gradual increases in anodic current, one from ca. 0.5 to 0.7 V and the other from ca. 0.8 to 1.0 V. It is quite possible that even at this stage, both α and β oxides, and possibly an intermediate (partially hydrated) state of this material, are present in the upper limit of the sweep. Certainly, in the region above 0.5 V, the anodic charge for oxide growth exceeded the cathodic charge for oxide reduction (the difference between the two may be attributed to a combination of hysteresis behavior and the difficulty of reducing β oxide species).

The effect of increasing the upper limit of the sweep to 1.5 V is illustrated in Fig. 1b. Note (a) the low potential (compared with most of the noble metals) for the onset of oxygen gas evolution, (b) the charge imbalance ($q_a > q_c$) above 0.5 V, and (c) the absence of a cathodic (H_{ads} formation) peak at ca. 0.26 V. Apparently, even at this stage (a single cycle), the anodically generated oxide film is difficult to reduce and the residual oxide impedes the formation of strong adsorbed hydrogen.

The response for a β-oxide-coated iridium electrode in acid solution is shown in Fig. 2a. The major differences, compared with Fig. 1b, are the pair of broad charge storage peaks at ca. 0.97 V and a less well-defined reversible response at ca. 1.4 V. Note that, despite the presence of the relatively porous β oxide deposit, the hydrogen desorption peaks at ca. 0.1 and 0.26 V are still clearly evident in the positive sweep, while an increase in anodic current above 0.4 V (in this case leading to a maximum at 0.63 V) is again observed. The counterparts of these peaks at 0.63 and 0.26 V are absent in the negative sweep but the cathodic (evidently oxide reduction) current response is unusually large over the range 0.6 to 0.3 V.

Attempts to grow thick multilayer β oxide films on iridium in acid solution at 75 °C by potential cycling were not successful; this is useful as it enables the response for the α oxide reaction to be observed more clearly. As shown by the full line in Fig. 2b, the reduction of such a deposit occurred in a rather sluggish manner, giving rise to a broad cathodic maximum in the negative sweep at ca. 0.34 V. It is apparently quite difficult to reduce all the oxide present at the interface (formed either on exposure of the surface to air or to potential cycling) even at 25 °C; note the extremely low anodic current at ca. 0.45 V in the positive sweep in Fig. 2a (apparently, the anodic double layer charging current in this region is almost cancelled out by the residual oxide reduction current) and the cathodic response below 0.4 V in the positive sweep at 75 °C, dashed line in Fig. 2b. The response for an iridium electrode coated with a β oxide film (grown, as in Fig. 2a, by potential cycling at 25 °C) in acid at 75 °C is shown by the dashed curve in Fig. 2b. In the region above 0.4 V, the anodic charge in the positive sweep is significantly greater than the cathodic charge in the negative sweep. Also, the magnitude of the anodic peak at ca. 0.95 V is much greater than that of its cathodic counterpart; such behavior was reported earlier [24] and was attributed to the poor electronic conductivity of the Ir (III) β oxide deposit.

Changing the electrolyte from sulfuric to perchloric acid makes little difference to the behavior of the electrode system. Examples are shown in Fig. 3a of cycles recorded

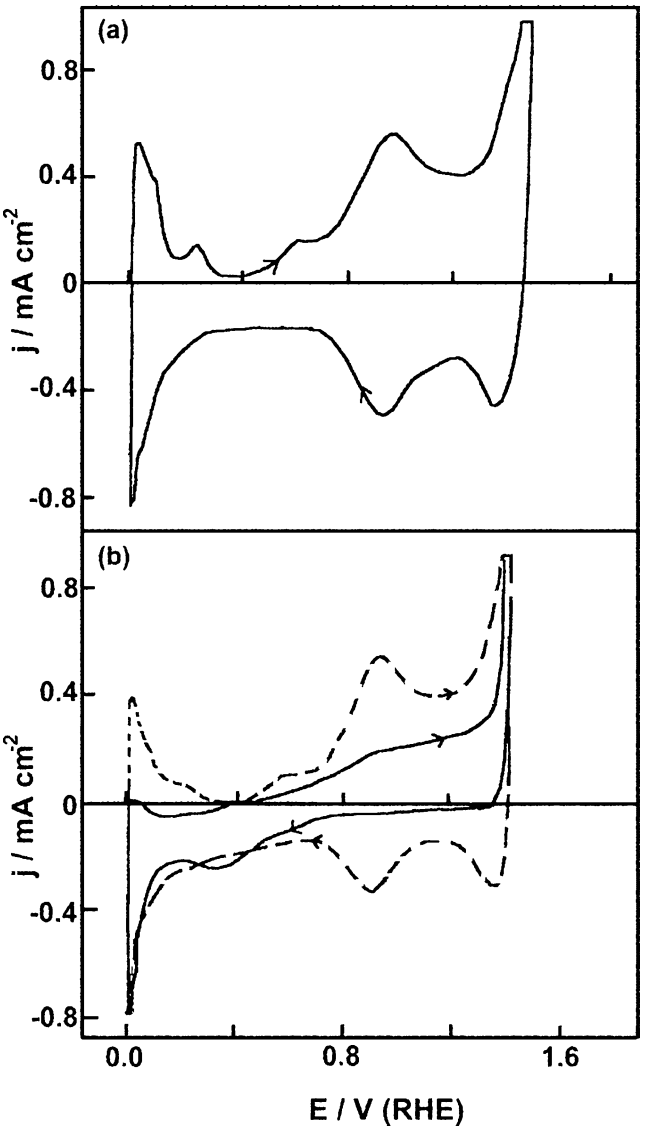

Fig. 2 Cyclic voltammograms (0.0 to 1.5 V, 50 mV s^{-1}) for iridium in 1.0 mol dm^{-3} H_2SO_4. **a** The electrode was coated with a hydrous oxide film grown in situ by repetitive cycling (60 cycles, 0.0 to 1.5 V, 0.1 V s^{-1}), T=25 °C. **b** *Full line*, repeat of (**a**) for a cell temperature of 75 °C (in this case, hydrous oxide film growth was not observed); *dashed line*, repeat of (**a**) for a film grown at 25 °C. The scan shown here was recorded at a cell temperature of 75 °C

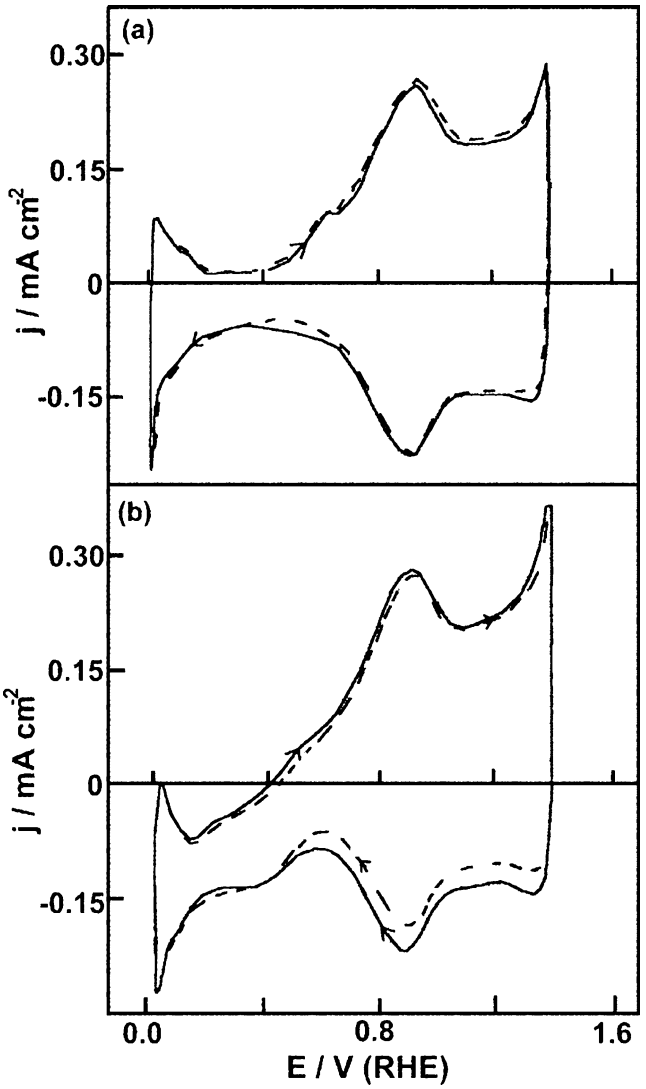

Fig. 3 Cyclic voltammograms (0.0 to 1.4 V, 50 mV s^{-1}) for hydrous oxide coated iridium electrodes in 1.0 mol dm^{-3} $HClO_4$ (120 cycles, with oxide growth conditions similar to those described in Fig. 2a). **a** *Full line*, response for a freshly grown oxide deposit at 25 °C; *dashed line*, response for the same electrode after cathodization at −0.4 V for 1.0 h. **b** Repeat of (**a**) except that the cell temperature was 75 °C and the cathodization was carried out for 1.0 h at −0.3 V

for a β-oxide-coated iridium electrode in $HClO_4$ solution at 25 °C before (full line) and after (dashed line) polarization at −0.40 V for 1.0 h; during this polarization period, the hydrogen gas evolution current decayed from 278 to 73 mA cm^{-2}. Such extended cathodization had very little effect on the voltammetric response; in particular, there was no obvious sign of a reduction of the main charge storage peaks at ca. 0.93 V (or in the charge storage capacity of the film over the range 0.6–1.4 V).

Similar β oxide charge storage data is shown in Fig. 3b for iridium in $HClO_4$ solution at 70 °C. As in H_2SO_4 solution at elevated temperature, dashed line in Fig 2b, the response below 0.4 V in the positive sweep was predominantly in the cathodic direction; this is attributed to a slow oxide reduction reaction. However, as indicated by the dashed line response in Fig. 3b, the vast majority of the β oxide deposit remained intact, with little change in its charge storage behavior, even after cathodization at −0.3 V for 1.0 h at 70 °C.

Behavior of β oxide films in aqueous base media

A cyclic voltammogram for a β-oxide-coated iridium electrode in base is shown by the full line in Fig. 4a. The main charge storage peaks (E_a=0.64 V, E_c=0.54 V)

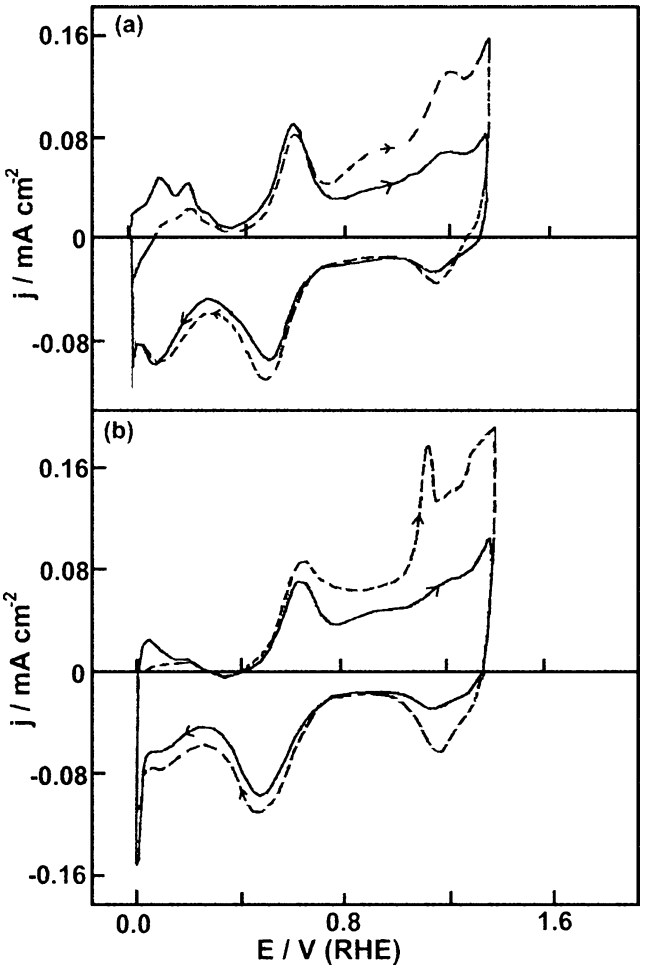

Fig. 4 Cyclic voltammograms (0.0 to 1.4 V, 50 mV s^{-1}) for a hydrous-oxide-coated iridium electrodes in 1.0 mol dm^{-3} NaOH (the oxide was grown in base at 25 °C,150 cycles, 0.0 to 1.5 V, 50 mV s^{-1}). **a** *Full line*, response for a freshly grown oxide deposit at 25 °C; *dashed line*, responses for the same electrode after cathodization at −0.2 V for 1.0 h. **b** Repeat of (**a**) except that the cell temperature was 50 °C and the cathodization was carried out at −0.3 V for 1.0 h

occurred (as pointed out earlier [25]) in this case at a lower potential than in acid; a less well-defined pair of peaks is evident at ca. 1.2 V. A curious feature in this case is the quite small anodic peak at ca. 1.1 V; this response (which lacks a cathodic counterpart) appeared in much more enhanced form in the first cycle, dashed line in Fig. 4b, recorded after extended cathodization at elevated temperature in base. Several hydrogen desorption peaks (E_p≈0.11, 0.21, and 0.29 V) appeared in the positive sweep, full line in Fig. 4a. The corresponding cathodic responses (below 0.3 V, negative sweep) were not well resolved; the cathodic charge under the broad peak at ca. 0.1 V in the negative sweep greatly exceeded its anodic equivalent; evidently, hydrogen adsorption was not the only process involved (it was apparently accompanied by sluggish oxide reduction).

Extended cathodic polarization of the β-oxide-coated electrode in base at 25 °C resulted in only a slight decrease in the charge storage response at ca. 0.6 V, Fig. 4a. In the same type of experiment in base at 50 °C, Fig. 4b, the peak responses at ca. 0.6 V were slightly enhanced after cathodization. It appears that β oxide deposits in general, in both base and acid, are quite reluctant to undergo reduction even on prolonged cathodization at potentials well below 0.0 V.

The data shown in Fig. 4a indicate that prolonged cathodization results in severe drop in the hydrogen adsorption capacity of the iridium surface (note the large decrease in anodic charge over the range 0.05 to 0.4 V, positive sweep); a corresponding drop in the hydrogen gas evolution rate in the course of extended cathodization was also observed (Figs. 5 and 6). Extended cathodization in base also significantly enhanced the anodic response above 0.7 V in the first positive sweep, Fig. 4; the effect on the negative sweep was less dramatic, and after a few cycles, the overall response was quite similar to that of the fresh, uncathodized, β-oxide-coated iridium electrode.

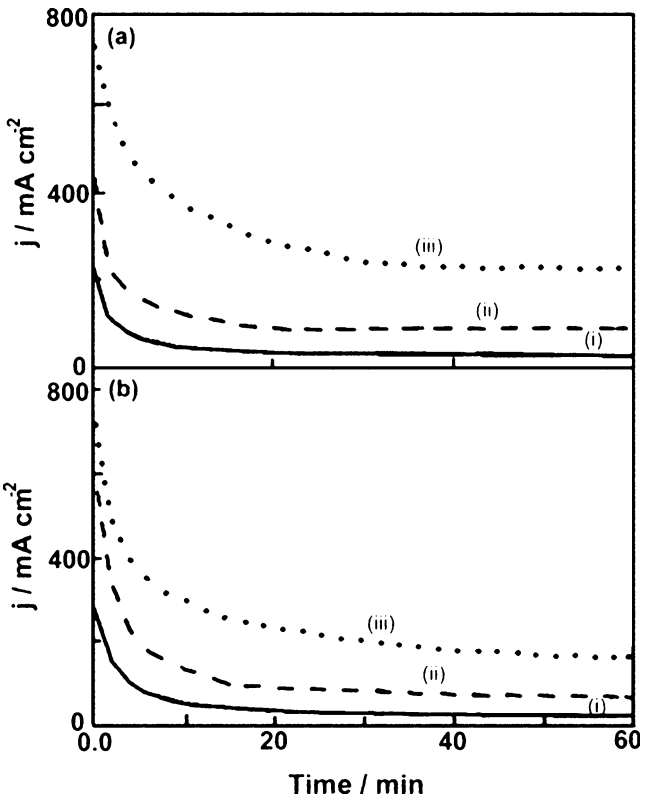

Fig. 5 Examples of hydrogen gas evolution decay plots for an iridium electrode in 1.0 mol dm^{-3} H_2SO_4 at 25 °C. In both cases, (i), (ii), and (iii) correspond to potentials of −0.2, −0.4, and −0.6 V, respectively. **a** Hydrous-oxide-free surface and **b** hydrous-oxide-coated surface (the oxide growth conditions for the latter in the acid solution were 120 cycles, 0.0 to 1.5 V, 50 mV s^{-1})

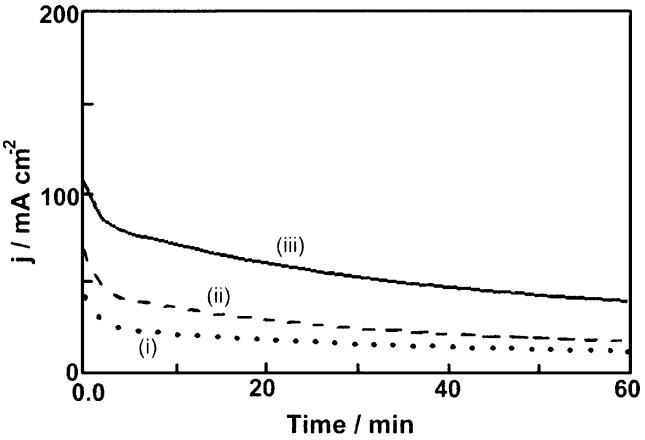

Fig. 6 Hydrogen gas evolution decay plots for hydrous-oxide-coated iridium electrodes in 1.0 mol dm^{-3} NaOH at 25 °C (oxide growth conditions in base solution were 240 cycles, 0.0 to 1.5 V, 50 mV s^{-1}): applied potentials: (i) −0.2 V, (ii) −0.3 V, and (iii) −0.4 V

Hydrogen gas evolution on iridium

The variation of the hydrogen gas evolution rate with the time, at a series of different potentials, is shown for a β-oxide-free, Fig. 5a, and a β-oxide-coated, Fig. 5b, iridium electrode in acid solution. In all cases, but especially at higher overpotentials, the rate of gas evolution decreased with time. This is not unusual as similar behavior was reported earlier [26] for gold in aqueous media. The trends with regard to current decay behavior were rather similar for both types of electrodes. However, the rate of decay was faster in the initial stages with β-oxide-coated iridium, and the rate of gas evolution after 60 min of cathodization at a constant potential was also slightly lower, compared with the bare metal, with this type of electrode. As illustrated in this study in Fig. 3, extended cathodization, even at −0.6 V for 60 min, resulted in very little change in the charge storage behavior of the interface, i.e., significant reduction of the β oxide film was not observed.

As outlined in Fig. 6, the hydrogen gas evolution responses for β-oxide-coated iridium electrodes in base were rather similar to those observed, Fig. 5b, for the same type of surface in acid. For a given potential, the initial current density values were generally lower in base but the same type of prolonged rate decay with time was observed for both acidic and basic media.

Behavior of thermally prepared IrO_2 deposits

An interesting difference was noted between titanium-supported RuO_2 and IrO_2 electrodes with regard to their responses in hydrogen (P=1.0 atm) saturated acid solution. Under such conditions, the RuO_2-coated electrodes yielded a steady-state open-circuit potential of ca. 0.8 V (RHE), while the IrO_2-coated electrodes yielded a value of ca. 0.0 V (RHE), i.e., the IrO_2 surface apparently behaved in a catalytic manner with respect to the hydrogen electrode reaction.

A typical cyclic voltammogram for a thermally prepared Ti-supported IrO_2 deposit in acid solution is shown by the full line in Fig. 7a. In the positive sweep, a substantial anodic background current was observed over the entire potential range. Poorly defined anodic peaks were noted, one at ca. 0.27 V and another, which was very ill-defined, at ca. 1.0 V. The corresponding cathodic maxima on the negative sweep occurred at ca. 0.86 and 0.07 V, respectively, and hydrogen gas evolution commenced at ca. 0.0 V. While IrO_2 films are quite active substrates for hydrogen gas evolution in acid, the deposit seemed to lack the long-term stability required for sustained operation. The dashed line in Fig. 7a shows that after 2.0 h of cathodization at −0.20 V (during which the current density decayed from 630 to 550 mA cm^{-2}), the voltammetric charge for the oxide film (which, as in the case of RuO_2 [10, 22], is assumed to be proportional to the mass of the deposit) exhibited a substantial decrease.

In contrast to the behavior observed with iridium metal, the rate of hydrogen gas evolution on IrO_2 deposits in acid solutions showed no indication of a rapid initial decay with time under constant overpotential conditions. Usually, the rate of evolution remained constant for at least 30 min; indeed, at an overpotential of −0.03 V, the cathodic current density rose from ca. 78 to 88 mA cm^{-2} during this initial 30-min period probably due to limited hydration of the outer region of the oxide film (as outlined earlier for RuO_2 [10, 11]). However, as summarized in this study in Table 1,

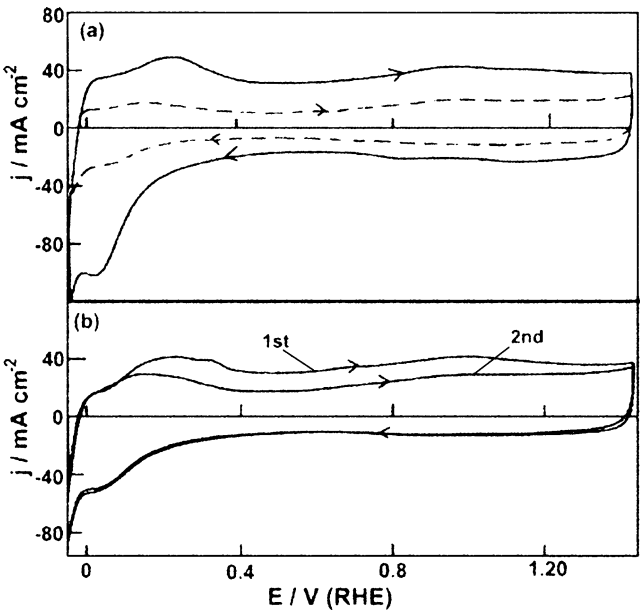

Fig. 7 Cyclic voltammograms (0–1.5 V at 20 mV s^{-1}) for an IrO_2-coated titanium electrode (annealed at 550 °C) in 1.0 mol dm^{-3} H_2SO_4 at 25 °C. **a** Fresh electrode (*full line*) and after cathodization at −0.25 V for 2 h (*dashed line*). **b** First and second sweeps after cathodization

Table 1 Decrease in hydrogen gas evolution activity for an IrO_2-coated electrode in 1.0 mol dm^{-3} H_2SO_4 at 25 °C

	Values				
η (V) (RHE)	−0.03	−0.08	−0.13	−0.18	−0.23
$j_{t=0}$ (mA cm^{-2})	90	200	340	485	630
$j_{t=2.0}$ (mA cm^{-2})	60	168	290	420	550

The current density values were taken at various potentials (line 1) before ($j_{t=0}$) and after ($j_{t=2.0}$) 2 h of cathodization at −0.25 V

after extended use as a cathode (2.0 h at −0.25 V), the hydrogen evolution performance of thermally prepared IrO_2 coatings (examined at a range of overpotentials before and after cathodization in acid solution) showed a significant decay. The first positive sweep recorded after extended cathodization was unusual. As shown in Fig. 7b, the anodic current over most of this sweep was abnormally large compared with later sweeps for the same electrode. The cathodic current in the negative sweep showed virtually no variation on postcathodization cycling, while after the first positive sweep, the anodic current response also remained constant for repeated cycles.

A typical cyclic voltammogram for a fresh thermally prepared IrO_2-coated electrode in base is shown in Fig. 8a. In the positive sweep, a significant increase in anodic current commenced at ca. 0.40 V; this was followed by an unusually broad peak over the range 0.4 to 1.2 V, which

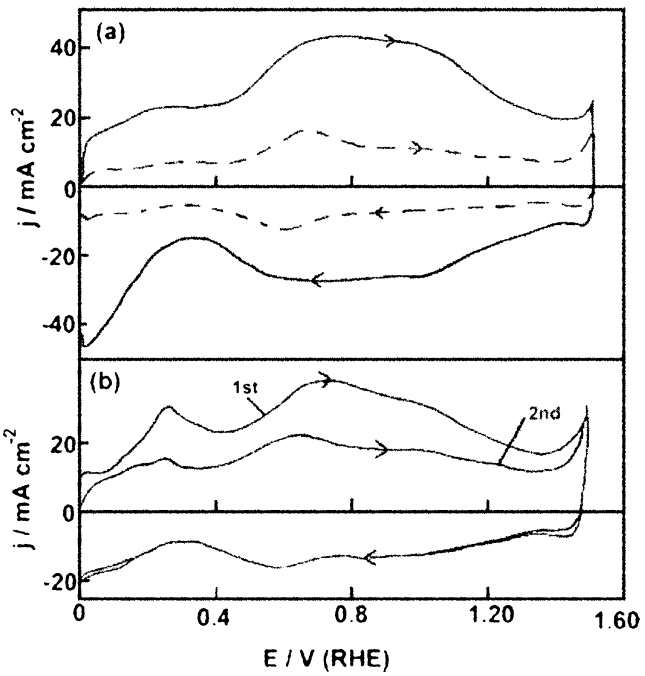

Fig. 8 Cyclic voltammograms (0–1.5 V at 20 mV s^{-1}) for an IrO_2-coated titanium electrode (annealed at 550 °C) in 1.0 mol dm^{-3} NaOH at 25 °C. **a** Fresh electrode (*full line*) and after cathodization at −0.25 V (RHE) for 8 h (*dashed line*). **b** First and second sweeps after cathodization

had a similarly broad cathodic counterpart in the subsequent negative sweep. As in acid, there was a small anodic feature at ca. 0.25 V (which was quite broad for IrO_2 in base) in the positive sweep and again a marked cathodic response below 0.3 V in the negative sweep.

IrO_2 deposits were quite active for hydrogen gas evolution in base, though not as effective as in acid. As illustrated in Table 2, the initial hydrogen evolution activity of IrO_2 in base was significantly greater than that of RuO_2 or RhO_2. However, in contrast to RuO_2, whose activity for gas evolution increased initially with time (as the outer layers of the deposit underwent hydration [10, 11]), the rate of gas evolution, at constant overpotential, on IrO_2 decayed quite significantly with time, Fig. 9 (the decay in question is also evident in the data shown in Table 2).

The origin of the hydrogen evolution current decay in base (as in acid) is attributed to a gradual loss of the oxide deposit; evidence for such loss is provided in Fig. 8a from which it is clear that extended cathodization is accompanied by a substantial decrease in surface voltammetric charge. As in acid, the first positive sweep recorded after prolonged cathodization was unusual; as shown in Fig. 8b, the anodic charge in this sweep was abnormally large. The responses for the negative sweeps were virtually invariant, as were those for the positive sweeps after the first. An interesting feature of the steady-state response in Fig. 8b is the presence of a pair of peaks at ca. 0.6 V; this is the region where hydrous (β) Ir oxide films in base exhibit their reversible charge storage behavior, Fig 4a.

The kinetics of hydrogen gas evolution at IrO_2-coated cathodes in aqueous acid media have been examined by a number of groups [12, 13, 38, 39]. A typical Tafel plot obtained in the present investigation is shown in Fig. 10; the slope in the region just below −0.4 V (SCE) is ca. 30 mV $decade^{-1}$. This aspect of IrO_2 electrochemistry was not investigated in detail as the behavior of high surface area cathodes for gas evolution reactions is complicated by electrode shielding effects plus gas trapping in pores. A number of authors [11, 12, 40] have pointed out that IrO_2 is more active than RuO_2 for hydrogen evolution, but reliable Tafel slope values are difficult to obtain for these oxide

Table 2 Variation of the hydrogen gas evolution rate with the nature of the Ti-supported oxide film in 1.0 mol dm^{-3} NaOH at 25 °C, η=−0.25 V

Film material	IrO_2	RuO_2	RhO_2
$j_{t=0}$ (mA cm^{-2})	390	240	170
$j_{t=2.0}$ (mA cm^{-2})	250	310	–

The rates refer to fresh electrodes ($j_{t=0}$) and in the case of both IrO_2 and RuO_2 to the values ($j_{t=2.0}$) observed after 2.0 h of cathodization at −0.25 V; all the oxide deposits were prepared from the appropriate chloride salts as outlined here for IrO_2

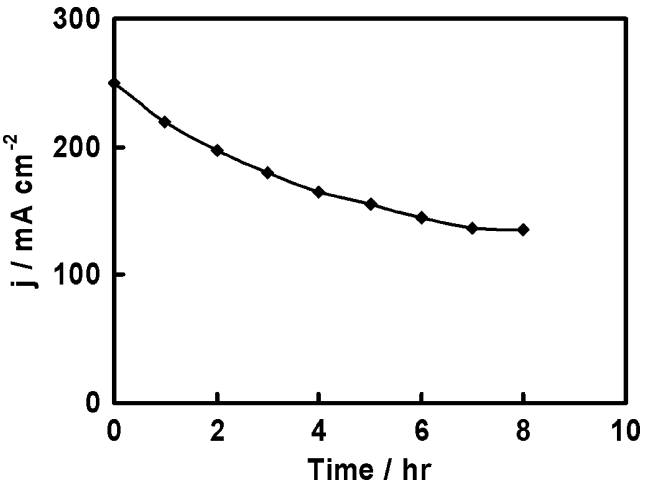

Fig. 9 Current decay plot for an IrO_2-coated titanium electrode (annealed at 550 °C) in 1.0 mol dm^{-3} NaOH at 25 °C; applied cathodic potential=−0.25 V

cathodes [13]. Some authors [38] have interpreted the cathodic behavior of IrO_2 in terms of a single Tafel plot (complicated at high overpotentials by ohmic drop effect), while others [12], who employed iR correction, have postulated the presence of two Tafel slopes, i.e., a change in mechanism, or rate-determining step, with increasing overpotential.

Discussion

Basic response for an iridium surface in aqueous acid solution

Iridium has a greater number of d-band vacancies than platinum [27] and therefore is assumed to be a stronger chemisorber and more susceptible to oxidation. This stronger interaction of iridium with oxygen is reflected in this study in the surface oxidation reaction which commences in acid solution, Fig. 1a, at ca. 0.5 V, as compared with ca. 0.85 V for a platinum surface under similar conditions [1]. Early cyclic voltammetry data reported for iridium needs to be viewed with caution as the distinction between monolayer and hydrous oxide film responses was not always appreciated and the reported behavior often appears to relate to composite films, i.e., a combination of α and β oxide species whose electrochemical properties are quite different.

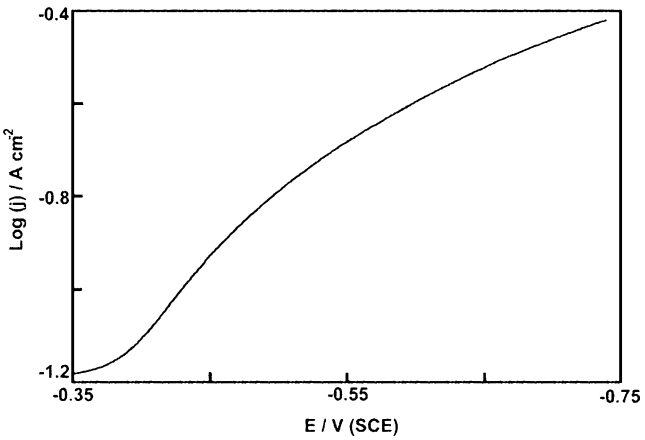

Fig. 10 Tafel plot for hydrogen gas evolution at an IrO_2-coated Ti electrode (annealed at 550 °C) in 1.0 mol dm^{-3} H_2SO_4 at 25 °C. Tafel slope at ca. −0.4 V (SCE) was ca. 30 mV $decade^{-1}$

There is a further problem with iridium in that the monolayer oxide reduction reaction is often quite sluggish, especially when the upper limit of the sweep is high. It is evident for instance in both sweeps in Fig. 1 that the anodic charge above 0.4 V in the positive sweep significantly exceeds the cathodic charge over the same region of the negative sweep. It is assumed that there are a number of contributions to this charge imbalance (which was discussed earlier by Vetter [28] for platinum in acid), e.g., (1) subsurface oxygen formation (in the first positive sweep, some of the anodically produced oxygen species enter the outer layers of the metal lattice [29], especially at defect sites); such species are not readily reduced, (2) the monolayer oxide species may only undergo partial reduction [28] in the region above 0.4 V in the negative sweep, e.g., IrO_n may reduced to $Ir(OH)_n$ species, the reduction of $Ir(OH)_n$ being sluggish, and (3) the oxide formed in the positive sweep is a mixture of monolayer and hydrous oxide species (reduction of the latter, as discussed in this study later, is extremely difficult even at E<0.0 V). There is a hint of a reversible transition at ca. 1.0 V in Fig. 1b, which is characteristic of the hydrous oxide charge storage reaction [9, 30]. Also, the peak for formation of strongly bound hydrogen, at ca. 0.26 V in the negative sweep in Fig. 1a, is absent in Fig 1b; evidently, some of the oxides formed at the upper limit of the sweep in the latter case are not reduced at 0.26 V and hence, there are few free sites available to accommodate strongly bound hydrogen.

The data shown in this study in Fig. 1 for iridium in acid at 25 °C are in reasonable agreement with the results of Rand and Woods [31]. A clear monolayer oxide reduction response is not easily observed for this system; the best example of the response for such a reaction (a cathodic peak with a maximum at ca. 0.35 V) is shown in the full line response in Fig. 2b. This relates to a cell temperature of 75 °C, but even in this study, sluggish oxide reduction is indicated by the small cathodic response over the range 0.05 to 0.4 V in the positive sweep.

Hydrous (or β) oxide responses for iridium in aqueous solution

The presence of a hydrous oxide deposit (produced by repetitive potential cycling) on the iridium electrode

involved in the case of Fig. 2a is clear from the large reversible charge storage response at ca. 1.0 V (the nature of this response and its variation with solution pH were discussed earlier [9]). An interesting feature of the system (pointed out earlier by Rand and Woods [31]) is that the presence of the hydrous oxide film, which is assumed to be of porous character, does not have a severe adverse effect on the adsorption of hydrogen by the iridium surface; the hydrogen desorption peaks below 0.4 V still appear in the positive sweep in Fig. 2a. Although the attempts to grow a multilayer hydrous oxide film in acid solution at 75 °C were not successful, Fig 2a, the film grown at 25 °C was relatively stable, and redox active, at the elevated temperature. The inability to grow the film at 75 °C may be due to rapid loss of an active state hydrous oxide precursor, e.g., iridium adatoms, which may either dissolve or agglomerate to a less reactive form before their conversion to the oxide. A further interesting point regarding the dashed line in Fig. 2b, and the responses shown in Fig. 3b, is the asymmetry of the charge storage peaks at ca. 0.9 V; the cathodic response is of lower magnitude than the corresponding anodic response (this is especially noticeable for cycles recorded at 75 °C). Such behavior supports the claim by Glarum and Marshal [32] that the reduced, Ir(III), form of the hydrous oxide couple is a poor electronic conductor, i.e., all the Ir(IV) species generated above 0.4 V in the positive sweep are not reduced rapidly in the same region of the negative sweep. Sluggish reduction of residual oxidized species continues at low potentials (E<0.4 V) even in the positive sweep in Fig. 3b. This conductivity barrier is assumed to be relevant even in cycles carried out at a cell temperature of 25 °C, e.g., in Fig. 2a, the anodic current (positive sweep) at 0.4 V is far lower than the cathodic current (negative sweep) at the same potential.

Some of the most remarkable results obtained in the present investigation are shown in Figs. 3 (for acid solution) and 4 (for base). The oxide films involved in these experiments (at least above ca. 0.5 V) are assumed to be of duplex character, i.e., an inner monolayer oxide deposit at the iridium surface and an outer coating of porous hydrous oxide material. The two layers are assumed to behave largely in an independent manner, i.e., inner film is extremely thin and its behavior was summarized in this study in terms of the response shown in Fig. 1a. The outer hydrous oxide layer is of porous character and quite reactive (it displays reversible charge storage properties, accompanied by an electrochromic effect [9]). The remarkable result is that such β oxide films can sustain quite high negative potentials (−0.4 V for 1 h in the case shown in Fig. 3a) without losing the hydrous oxide charge storage response. This is not a totally novel observation; in his review of the surface electrochemistry of the noble metals, Woods [1] pointed out (p. 106) that "the sizes of the oxygen peaks [for iridium] are unaffected by holding the electrode for long periods at potentials in the hydrogen-evolution region". These are remarkable results for a metal which, according to Pourbaix [21], has no bulk oxide stable below ca. 0.93 V (RHE).

The reluctance of hydrous oxide films to undergo reduction in aqueous media was pointed out earlier for Pt [33, 34], Ru [10], and Au [2, 35]. The cations in such a deposit, assumed in the present case to be predominantly Ir^{3+}, are apparently surrounded by a sphere of oxyligands, e.g., OH^- and OH_2 species. The barrier to reduction is assumed (as discussed earlier [10, 35]) to be that the primary products of the reaction are virtually isolated iridium atoms, $\mu^0[Ir(g)] = 617.98\ \mathrm{kJ\,mol^{-1}}$ [36]. Using Pourbaix's data [21] for hydrous Ir_2O_3(s) and assuming that the β oxide reduction reaction in acid solution (pH=0) may be represented as follows, viz.,

$$\begin{aligned} \mathrm{Ir_2O_3(hydr.) + 6H^+(aq) + 6e^- = 2Ir(g) + 3H_2O\ (l)} \\ \Delta\mu^0 = 2(617.98) + 3(-237.2) \\ -(175.7) = 700.1\ \mathrm{kJ\,mol^{-1}} \end{aligned} \quad (1)$$

$$E^0 = -\frac{\Delta\mu^0}{nF} = -\frac{(700.1)}{6(96.487)} = -1.21\ \mathrm{V(RHE)} \quad (2)$$

It is clear that the involvement of a very high-energy intermediate will strongly inhibit (as observed here) the reduction of the β oxide deposit. The low conductivity of the Ir(III) deposit is unlikely to be the source of inhibition of the reduction of the latter as this reaction should be able to progress outward from the metal surface (the resistance to reduction in the experiments outlined in Fig. 3 was quite marked; it was maintained over a polarization period of 1 h).

The β oxide charge storage peak occurs at ca. 0.6 V in base, Fig. 4; this shift in peak potential to lower values on increasing the solution pH is a common feature in hydrous oxide electrochemistry [9] and has been attributed to the anionic character of the oxyspecies present in multilayer surface deposits (the highly charged cations coordinate an excess of OH^- ions). As in acid solution, subjecting β-oxide-coated iridium electrodes to prolonged cathodization in the hydrogen evolution region resulted in no loss of the β oxide charge storage response (indeed, in this case, the response in question appeared to be slightly enhanced). The origin of enhanced responses above 0.6 V, especially in the positive sweep in Fig. 4b, is discussed in this study later.

Hydrogen gas evolution at iridium and β-oxide-coated iridium electrodes

While hydrogen gas evolution rates for both initially oxide-free, Fig. 5a, and β-oxide-coated, Fig. 5b, iridium electrodes in acid solution were quite high initially, there was a marked decay in rates with time at the three potential values investigated in this study. This is not unusual; similar behavior was reported earlier for gold in acid solution [26] and was recently observed in this laboratory for platinum in base. An interesting question in this study is whether the hydrogen evolution reaction, in the case of Fig. 5b, occurs at the β oxide surface, the underlying metal surface (beneath the porous oxide film), or on both types of sites. Because the reduced, Ir(III), form of the oxide is a poor conductor [32], it is assumed that the reaction occurred predominantly at the metal sites. However, some reductions of the Ir(III) oxide may occur at $E<0.0$ V, i.e., the film may have increased conductivity in the hydrogen evolution region due to the presence of Ir(II) centers in the Ir(III) β oxide deposit. In the case of Fig. 5, the initial rates of evolution in (a) and (b) were rather similar (for the same overpotential values), but the decay in the rate with time was faster (especially at −0.6 V) in the presence of the β oxide deposits.

The decay of the hydrogen evolution current with time under constant potential conditions was attributed earlier [26] to hydrogen activation of the metal surface. Gradual entry of hydrogen into the outer layers of the metal lattice (or metal hydride formation) causes rupture, subdivision, and activation of the metallic grains (basically, the surface metal atoms acquire energy under hydrogen gas evolution conditions). This may have two effects which would explain the decay in hydrogen evolution rate: (1) the activated surface state adsorbs intermediates, such as H_{ads}, less strongly (activated metal atoms tend to be strong electron donors [37] rather than d-band acceptors in the stable state); and (2) severe activation may eventually result in oxidation of surface metal atoms, oxide formation resulting in a severe drop in electrocatalytic activity for the hydrogen evolution reaction. The data summarized in this study in Fig. 3 demonstrates that, irrespective of conventional thermodynamic data (and assumptions base on the latter), hydrous Ir oxide species generated at an electrode/solution interface are quite reluctant to undergo reduction in the hydrogen evolution region.

Similar current decay curves were observed for hydrous-oxide-coated iridium in base, Fig. 6. The initial rate of evolution, e.g., at −0.4 V, was lower in base, as compared with acid, as (a) the initial reactant (H_3O^+ in acid, H_2O in base) is different, and (b) inhibiting oxide species are likely to be formed more readily at high OH^- ion activity. The increased anodic activity above ca. 0.6 V after prolonged cathodization (dashed lines in Fig. 4) may reflect oxidation of some cathodically activated iridium. However, there may also be a major contribution in this region due to the generation of Ir(VI) species. The latter may not be completely reduced under continuous cycling conditions, but such reduction to Ir(III) may be much more extensive on prolonged cathodization.

Hydrogen evolution at thermally prepared IrO_2 deposits

Detailed investigations of the behavior of IrO_2-coated cathodes operated under hydrogen gas evolution conditions have been reported by Trasatti and coworkers [22, 38, 39] and Guay and coworkers [12, 13, 23]; however, the attention of the latter group was concentrated more on RuO_2 which they investigated concomitantly. Some works have also been devoted to the use of mixed oxide (RuO_2 + IrO_2) coatings for hydrogen gas evolution [11, 13, 40]. As discussed earlier [10] for thermally prepared RuO_2 films and outlined in this study for hydrous β oxide deposits, these noble metal oxide coatings are thermodynamically unstable under hydrogen evolution conditions (these are highlighted also by other authors [38]); they may be classified as metastable metal oxide cathodes.

According to the present work, IrO_2-coated cathodes differ from their RuO_2 equivalent in two significant respects. The IrO_2 deposits were capable of equilibrating hydrogen, i.e., an $IrO_2/H_2/H_3O^+$ electrode gradually attained a potential of 0.0 V (RHE); such behavior was not observed [10] with RuO_2-coated electrodes. As illustrated in this study in Fig. 7a for acid and Fig. 8a for base, thermally prepared IrO_2 deposits lost charge capacity with use due to the gradual detachment of oxide particles. This loss of IrO_2 under severe hydrogen evolution conditions was evidently not observed in earlier work; however, it may be noted that Chabanier and Guay [23] reported a noticeable reduction in the IrO_2/Ti in situ X-ray absorption peak area ratio with polarization time. Such behavior, which was not observed with RuO_2 films, was permanent; because it was not apparently due to oxide reduction to metallic iridium [23], gradual detachment of IrO_2 microparticles seems to be a reasonable explanation.

The effect of the oxide annealing temperature on the cyclic voltammetry responses of IrO_2 films in base was reported by Chen and Trasatti (see Fig. 4 in their paper [22]). When the annealing temperature was low (330 °C), a conjugate pair of peaks, corresponding to a reversible redox transitions, was observed at ca. −0.42 V (SCE) which (for a pH of ca. 13.5) is equivalent to ca. 0.62 V (RHE). Evidently, the transition involved corresponds to the charge storage reaction of hydrous Ir oxide species (see the conjugate pair of peaks in the same potential region in Fig. 4 of the present work). When the annealing temperature was raised above 350 °C [22], the magnitude of the charge storage peaks

decreased dramatically, presumably as the reactive (easily hydrated) IrO_x species (produced by oxidation of $IrCl_3$) become trapped in a more extended, less reactive, rutile structure (or as the oxide underwent extensive sintering) at the higher annealing temperature.

A notable feature of the voltammetric response for fresh IrO_2 electrodes in both acid, Fig. 7a, and base, Fig. 8a, is the large reduction response below 0.2 V in the negative sweep; this is more marked in acid, and for the latter, there is a clear indication on an anodic counterpart at ca. 0.25 V in the positive sweep. Such responses occurred at potentials which are far too low to be attributed to an Ir(IV)/Ir(III) transition. They are probably due to a surface pseudocapacitance process, i.e., some degree of reduction of Ir(III) oxyspecies, the product acting a mediator system in the hydrogen gas evolution reaction (below 0.0 V) as discussed earlier [10] for RuO_2 cathodes under similar circumstances. The responses for postcathodized IrO_2 in base are interesting; the conjugate pair of peaks at ca. 0.65 V is clearly evident for instance in the dashed line in Fig. 8a. The corresponding response for the β oxide transition in acid, which should occur at ca. 1.0 V, is far less marked, Fig. 7.

It seems clear from the data shown in this study in Fig. 7b and Fig. 8b that the hydrogen evolution reaction occurs at a reduced oxide surface. The first positive sweep recorded after extended cathodization gave an abnormally large anodic response over most of the potential range. The extended nature of this response suggests that the process involved is due to gradual oxygen reinsertion; it seems, therefore, that the surface involved in hydrogen gas evolution, or H_2/H_3O^+ equilibration, is one of low oxygen stoichiometry and is significantly different from the bulk IrO_2 phase.

The IrO_2 (like the RuO_2 [10]) deposits are assumed to be high surface area particulate materials with relatively weak adhesion between the oxide particles. Changes in the oxide stoichiometry at low potentials, e.g., conversion of bridging oxygen to terminal oxygen, are assumed to result in gradual loss of contact and shedding of oxide particles, which were observed, after extended cathodization, on the floor of the cell. With these oxide electrodes, the voltammetric charge (under cyclic voltammetry conditions) is commonly regarded as a measure of the real surface area of the oxide film; hence, the drop in voltammetric charge after extended cathodization in acid, Fig. 7a, and base, Fig. 8a, is attributed to the loss of surface area due to shedding of oxide particles.

The decay in hydrogen gas evolution rate under constant potential conditions was much slower in the case of the thermal oxide (Fig. 9) as compared with the hydrous-oxide-coated iridium metal (Fig. 6). This is not surprising as in the former, the decay is attributed to the loss of oxide surface area, whereas in the latter, the effect is attributed to hydrogen-induced surface deactivation. It is possible, from a practical viewpoint, that the oxide shedding problem may be lessened by using a composite IrO_2/colloidal PTFE electrode system as is commonly used in the fuel cell area.

The Tafel plot for hydrogen gas evolution in base, Fig. 10, is quite similar to that reported earlier for RuO_2 under similar conditions [10]. In both cases, the region of rapid current density increase is quite short; the limiting value attained at an overpotential of ca. −0.6 V was ca. 0.5 A cm^{-2}. There are a number of complications that are likely to restrict the performance of these oxide cathodes, e.g., ohmic drop; gas bubble evolution is also likely to reduce the effective electrode area (this is assumed to be most marked in pores where gas evolution is likely to expel electrolyte), and the maximum turnover frequency at surface active sites may be limited. In view of the similarity of the Tafel plots for hydrogen gas evolution at IrO_2 (Fig. 10) and RuO_2 cathodes, the mechanism of the electrode reaction is assumed to be virtually identical.

Conclusions

1. The cyclic voltammetric behavior of iridium in aqueous media is complicated by the ability of the metal to form two distinguishable (α and β) surface oxide species. Hydrous (or β) oxide species are very reductant to undergo reduction even on prolonged exposure to hydrogen gas evolution conditions.
2. The rate of hydrogen gas evolution at iridium electrodes decays dramatically with time as the hydrogen activates the metal surface, resulting apparently in the oxidation (or hydrous oxide formation), and hence loss of catalytic activity, of surface active sites.
3. Thermally prepared IrO_2 films on titanium differ from their RuO_2 equivalents [10] in that the IrO_2 deposits were observed to equilibrate the H_2/H_3O^+ reaction and to shed oxide particles under sustained hydrogen gas evolution conditions; the latter resulted in a loss of oxide surface area and a decay in the hydrogen evolution rate under constant potential conditions.
4. The thermodynamic instability of noble metal oxide cathodes for hydrogen gas evolution was pointed out earlier by Boodts and Trasatti [38]; such behavior is interpreted here in terms of a barrier to oxide reduction due to the intervention of high-energy intermediate (microcluster) states of the metal.

References

1. Woods R (1976) Chemisorption at electrodes. In: Bard AJ (ed) Electroanalytical chemistry, vol 9. Marcel Dekker, New York, pp 1–162
2. Burke LD, Moran JM, Nugent PF (2003) J Solid State Electrochem 7:529

3. Burke LD, Ahern AJ, O'Mullane AP (2002) Gold Bull 35:3
4. Kolb DM, Schneeweiss MA (1999) Electrochem Soc Interface 8:26
5. Moffat TP (1999) Scanning tunneling microscopy studies of metal electrodes. In: Bard AJ, Rubinstein I (eds) Electroanalytical chemistry, vol 21. Marcel Dekker, New York, pp 252–255
6. Dieluweit S, Giesen M (2002) J Electroanal Chem 194:542–545
7. Burke LD (2004) Gold Bull 37:125
8. Burke LD, Hurley LM, Lodge VE, Mooney MB (2001) J Solid State Electrochem 5:250
9. Burke LD, Lyons MEG (1986) Electrochemistry of hydrous oxide films. In: White RE, Bockris JO'M, Conway BE (eds) Electroanalytical chemistry, no. 18. Plenum, New York, pp 169–248
10. Burke LD, Naser NS (2005) J Appl Electrochem 35:931
11. Kodintsev IM, Trasatti S (1994) Electrochim Acta 39:1803
12. Chen L, Guay D, Lasia A (1996) J Electrochem Soc 143:3576
13. Blouin M, Guay D (1997) J Electrochem Soc 144:573
14. Børresen B, Hagen G, Tunold R (2002) Electrochim Acta 47:1819
15. Lister TE, Tolmachev YV, Chu Y, Cullen WG, You H, Yonco R, Nagy Z (2003) J Electroanal Chem 17:554–555
16. Conway BE (1991) J Electrochem Soc 138:1539
17. Liu XM, Zhang XG (2004) Electrochim Acta 49:229
18. Yong-gang W, Xiao-gang Z (2004) Electrochim Acta 49:1957
19. Sugimoto W, Kizaki T, Yokoshima K, Murakami Y, Takusa Y (2004) Electrochim Acta 49:313
20. Conway BE (1999) Electrochemical supercapacitors. Kluwer/Plenum, New York
21. Pourbaix M (1966) Atlas of electrochemical equilibria in aqueous solutions. Pergamon, Oxford
22. Chen H, Trasatti S (1993) J Appl Electrochem 23:559
23. Chabanier C, Guay D (2004) J Electroanal Chem 570:13
24. Burke LD, Whelan DP (1984) J Electroanal Chem 162:121
25. Burke LD, Whelan DP (1981) J Electroanal Chem 124:333
26. Burke LD, O'Mullane AP, Lodge VE, Mooney MB (2001) J Solid State Electrochem 5:319
27. Burke LD (1980) Oxide growth and oxygen evolution on noble metals. In: Trasatti S (ed) Electrodes of conductive metallic oxides, part A. Elsevier, Amsterdam, pp 141–181
28. Vetter KJ (1967) Electrochemical kinetics. Academic, New York, p 620
29. Savinova ER, Kraft P, Pettinger B, Dobbhofer K (1997) J Electroanal Chem 430:47
30. Buckley DN, Burke LD (1975) J Chem Soc Faraday Trans 171:1447
31. Rand DAJ, Woods R (1974) J Electroanal Chem 55:375
32. Glarum SH, Marshall (1980) J Electrochem Soc 127:1467
33. Burke LD, Ahern AJ (2001) J Solid State Electrochem 5:553
34. Burke LD, Buckley DT (1994) J Electroanal Chem 366:239
35. Burke LD, O'Mullane AP (2000) J Solid State Electrochem 4:285
36. Wagman DD, Evans WH, Parker VB, Halow I, Bailey SM, Schumm RH (1969) NBS Technical Note 270-4: selected values of chemical thermodynamic properties. US Government Printing Office, Washington D.C. 20234, p 103
37. Henglein A (1995) Ber Bunsenges Phys Chem 99:903
38. Boodts JCF, Trasatti S (1989) J Appl Electrochem 19:255
39. Chen H, Trassati S (1993) J Electroanal Chem 357:91
40. Wen T-C, Hu C-C (1992) J Electrochem Soc 139:2158